Supplementary Figures

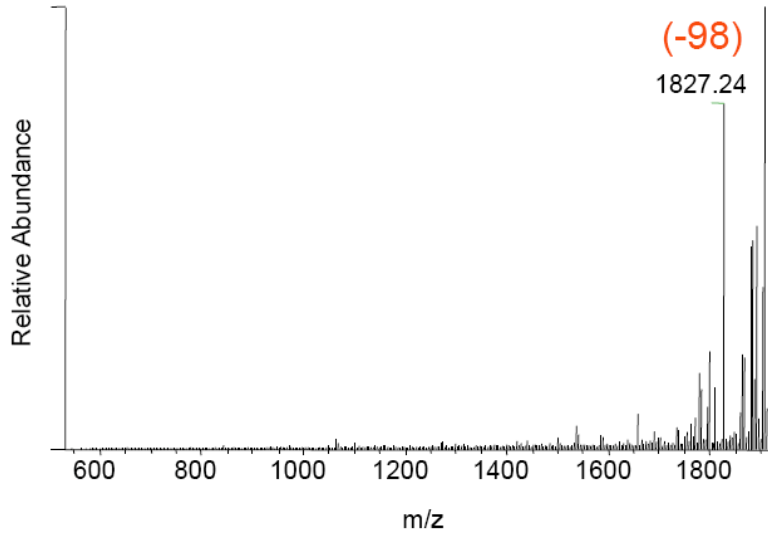| aa	m/z	Sequence and phosphorylated residue
35-45	1327.688	SHSNILKPPVR
35-50	1925.037	SHSNILKPPVRLDQLK
63-75	1542.768	YIQGGKEVSPTKR
210-237	3022.378	pyroQDSSDGENELNGGLGLFNEQGGLQQLIK
203-237	3793.863	LQSALLKQDSSDGENELNGGLGLFNEQGGLQQLIK
273-286	1732.710	PEGYSPFQQDDIEK
270-286	2091.894	PYVPEGYSPFQQDDIEK
266-286	2541.128	pyroQEPLPYVPEGYSPFQQDDIEK
289-295	936.386	TFNSPYK
296-322	3192.424	LDLEDEDDTPDKVDLLPLEQIDEEGEK

Supplementary Figure 1. Identities of securin phosphopeptides and phosphorylation sites were determined after analysis of tandem MS/MS and MS/MS/MS fragmentation spectra of tryptic peptides. At least ten MS/MS spectra exhibited a fragment corresponding to loss of 98 Da, a characteristic signature of a phosphopeptide. Further interpretation of the MS/MS/MS spectra of fragments of these phosphopeptides resulted in confirmation of peptide sequences and revealed the positions of phosphorylation sites. The table summarizes the sequences and phosphorylation sites of the ten phosphopeptides that were detected; subsequent panels provide the fragmentation spectra of each phosphopeptide in the order given in the table.

MS/MS 1327.688 m/z

y9 8 6 5 4

Pds1 [35-45]: SHpSNILKPPVR

(-98)

1229.58

Relative Abundance

y4

y5 y6

y8

y9

400   600   800   1000   1200

m/z

MS/MS/MS1 1229.58 m/z

z9 y8 4

Pds1 [35-45]: SHSNILKPPVR

b4 6 7

z9

1212.55

Relative Abundance

b4 y4

b6

b7

y8

-R

400   600   800   1000   1200

m/z

2
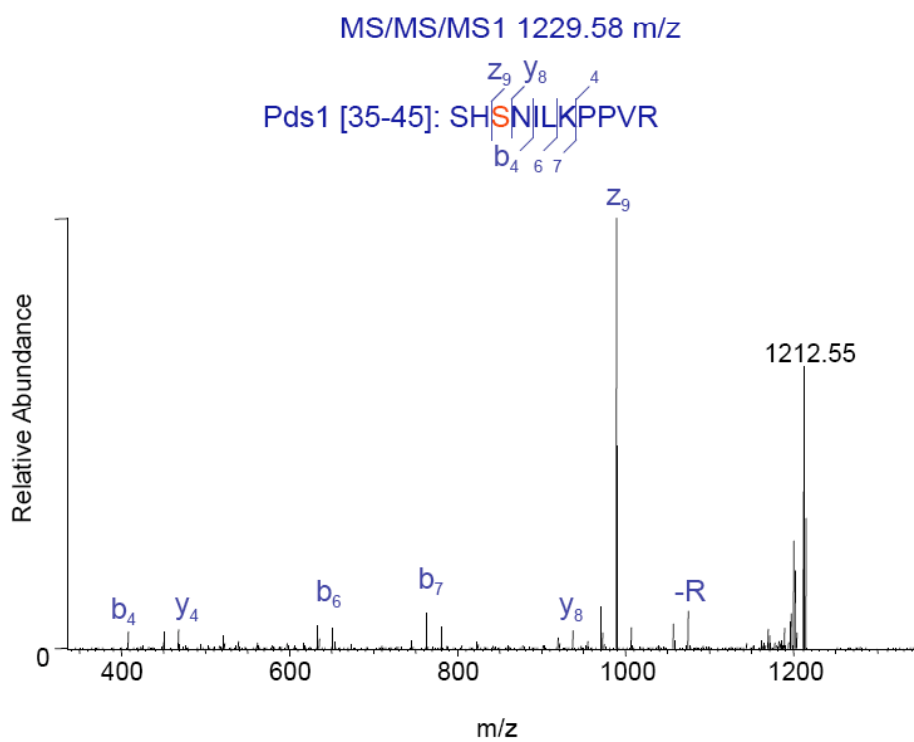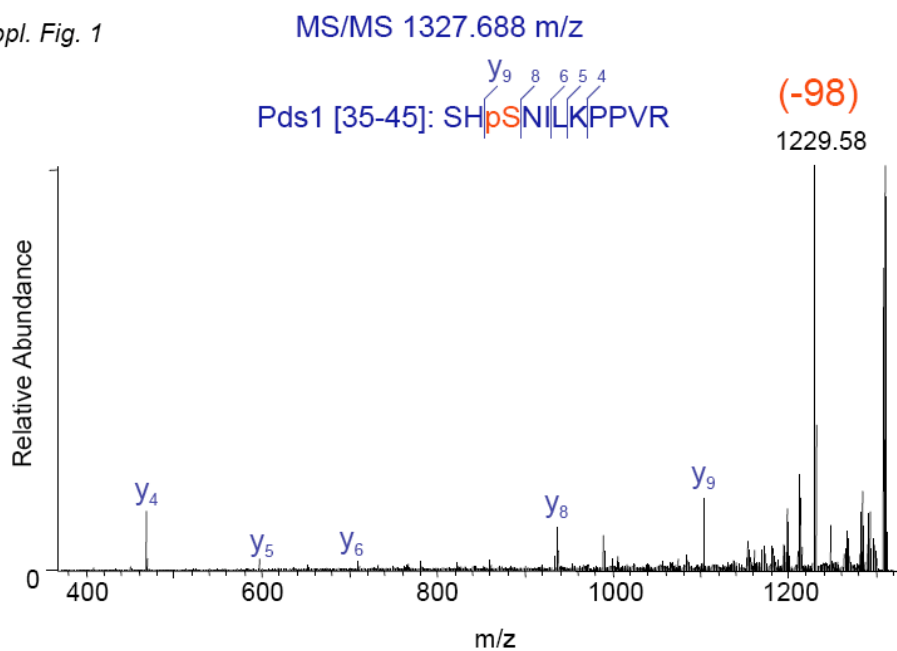
MS/MS 1925.037m/z

Pds1 [35-50]: SHpSNILKPPVRLDQLK

(-98)

1827.24

MS/MS/MS 1827.24 m/z

$y_{9\ 10}$

Pds1 [35-50]: SHSNILKPPVRLDQLK

$c_{13\ 14\ 15}$

c_{13}

c_{14}

c_{15}

y_9 y_{10}^{*}
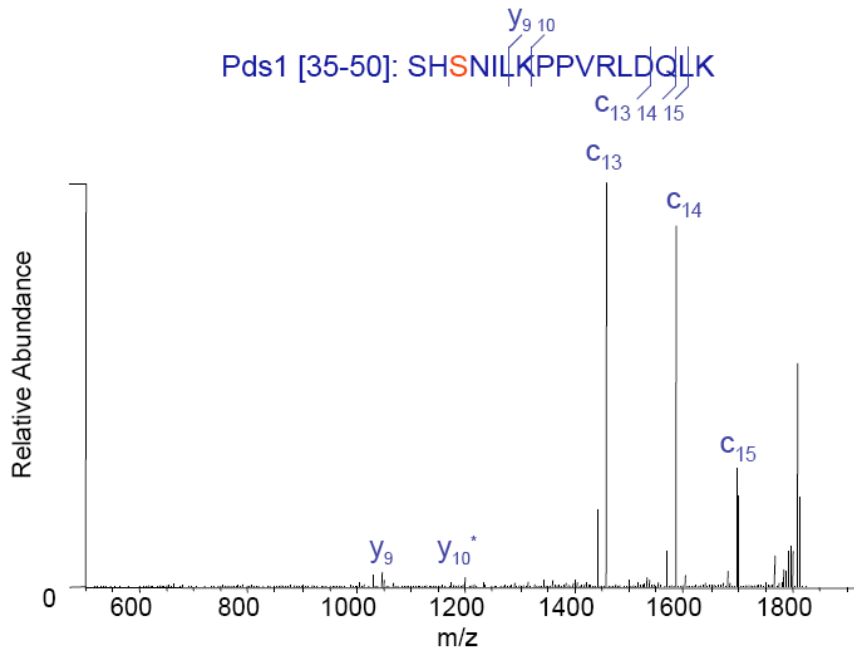
Suppl. Fig. 1

MS/MS 1542.768 m/z

Pds1 [63-75]: YIQGGKEVpSPTKR

(-98)
1444.82

1239.82
1353.00
1105.55
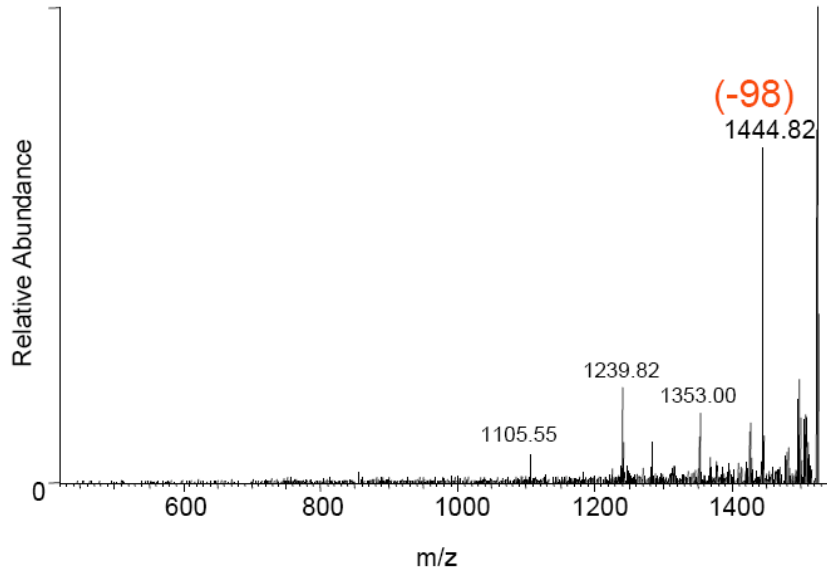
MS/MS/MS 1444.82 m/z

Pds1 [63-75]: YIQGGKEVSPTKR

y_{10} 7 6 5 4

b_8 10 11 12

b_{12}

-R

y_4 y_5 y_6 y_7 b_8 c_9 b_{10} y_{10} b_{11}
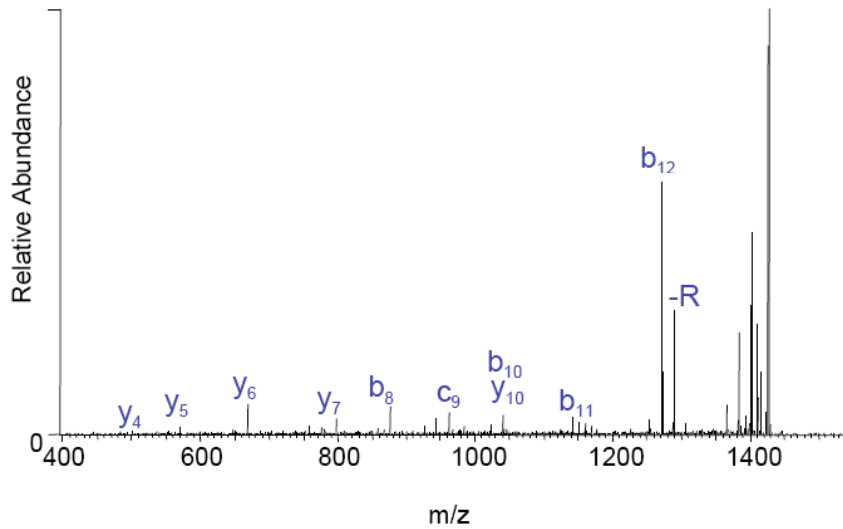
Suppl. Fig. 1

MS/MS 3022.378 m/z

Pds1 [210-237]: pyroQDpSSDGENELNGGLGLFNEQGGLQQLIK

MS/MS/MS 2925 m/z

Pds1 [210-237]: pyroQDSSDGENELNGGLGLFNEQGGLQQLIK

5

MS/MS 3793.863 m/z

y₂₃
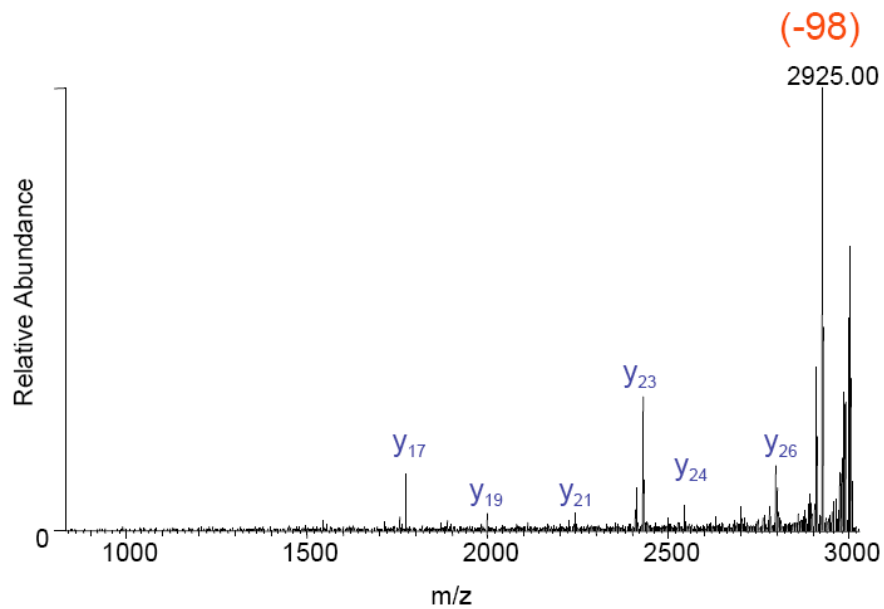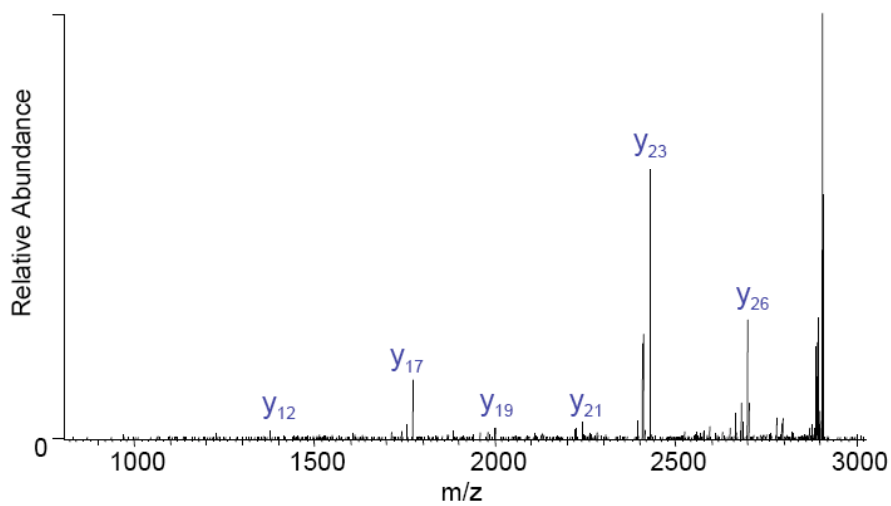
Pds1 [203-237]: LQSALLKQDpSSDGENELNGGLGLFNEQGGLQQLIK
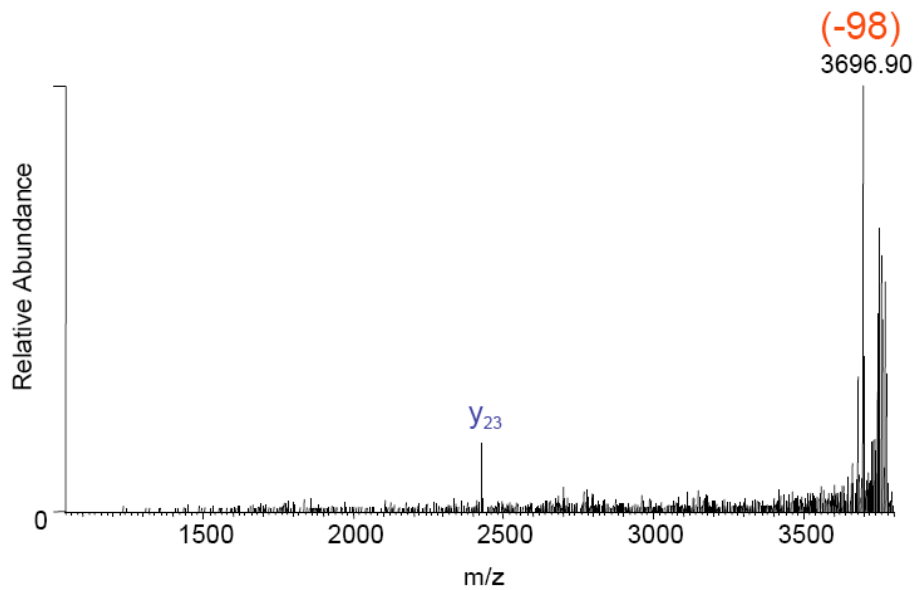
(-98)
3696.90
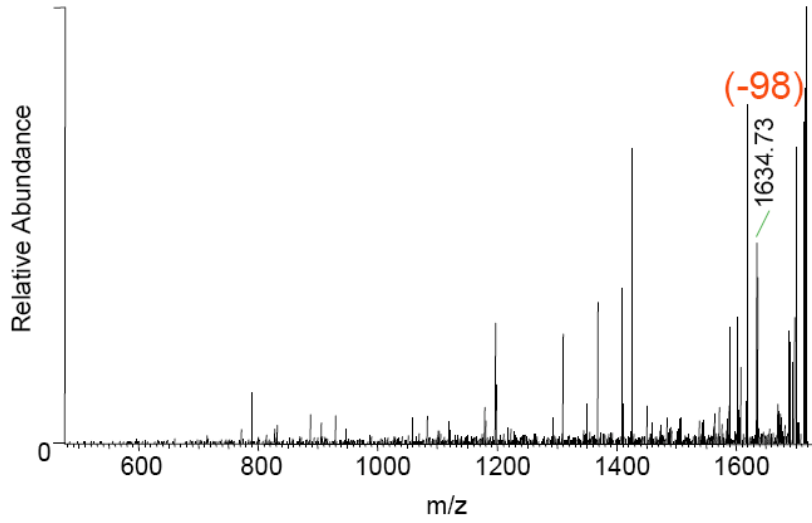
y23

MS/MS/MS 3796.90 m/z

y₂₆ 23 17

Pds1 [203-237]: LQSALLKQDSSDGENELNGGLGLFNEQGGLQQLIK

y23

y26

y17

6
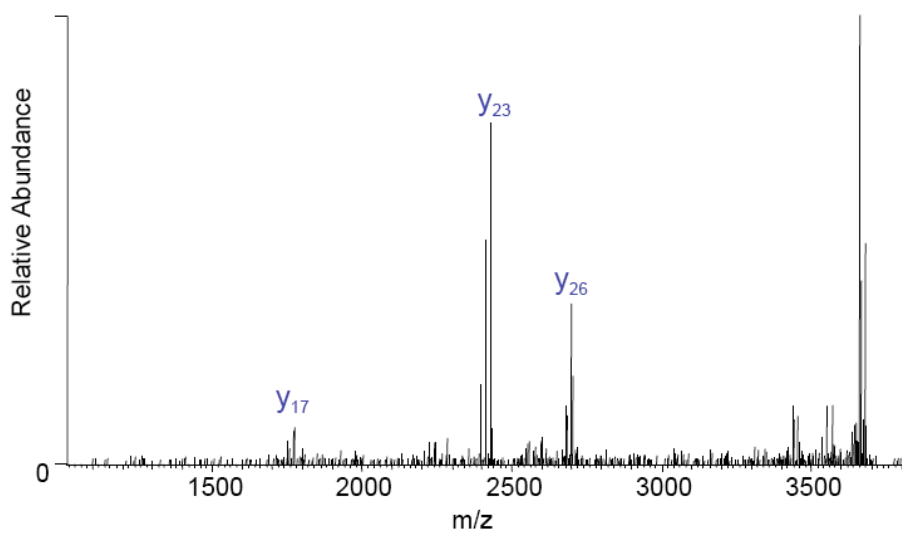
MS/MS 1732.710 m/z

Pds1 [273-286]: PEGYpSPFQQDDIEK

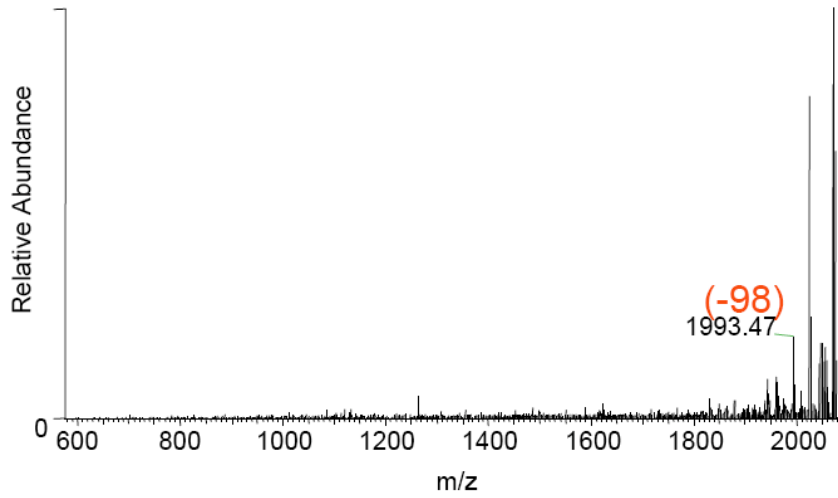MS/MS/MS 1634.73 m/z

Pds1 [273-286]: PEGYSPFQQDDIEK

7
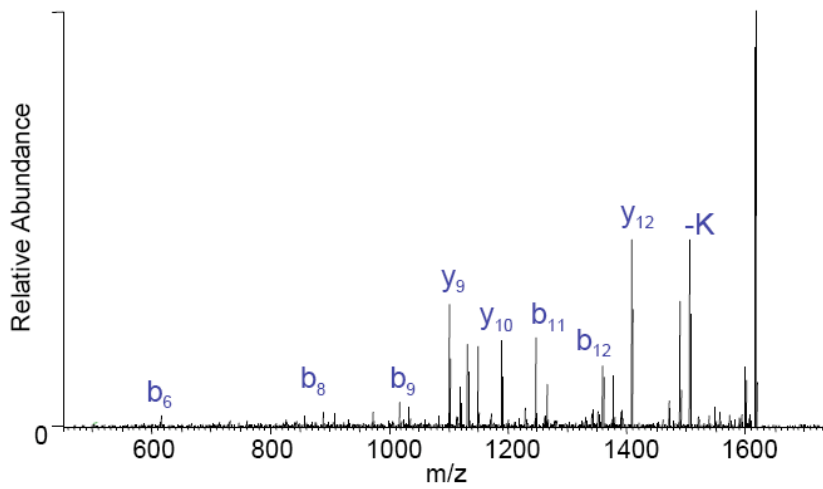
MS/MS 2091.894 m/z

Pds1 [270-286]: PYVPEGYpSPFQQDDIEK

(-98)
1993.47

MS/MS/MS 1993.47 m/z

y₁₅ ₁₄ ₁₂ ₁₀ ₉

Pds1 [270-286]: PYVPEGYSPFQQDDIEK

b₁₃

MS/MS 2541.128 m/z

Pds1 [266-286]: pyroQEPLPYVPEGYpSPFQQDDIEK

y16 14 13 12 9

MS/MS/MS 2443.75 m/z

Pds1 [266-286]: pyroQEPLPYVPEGYSPFQQDDIEK

y19 17 15 14 12

b9

Suppl. Fig. 1

MS/MS 936.386 m/z

Pds1 [289-295]: TFNpSPYK

(-98)
838.79

MS/MS/ 838.79 m/z

Pds1 [289-295]: TFNSPYK

$y_{5\ 4\ 3}$

b_6

y_5

y_3

z_4
y_4

b_6
-K
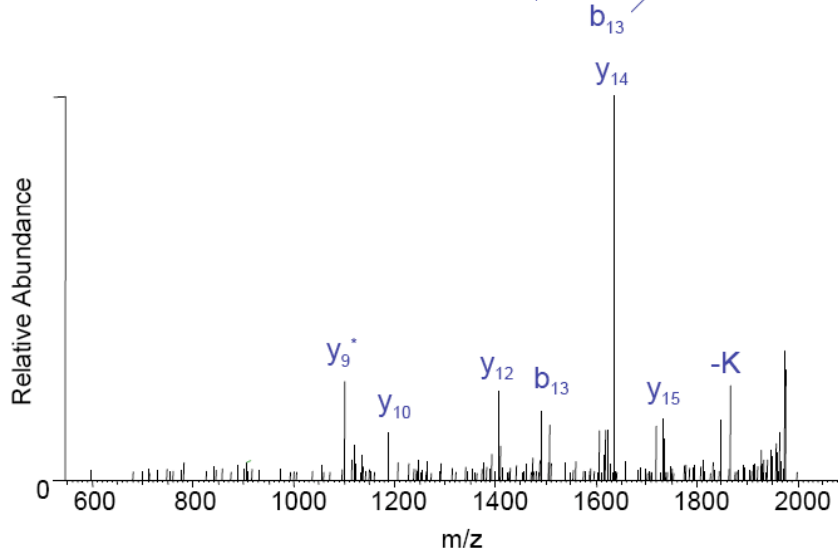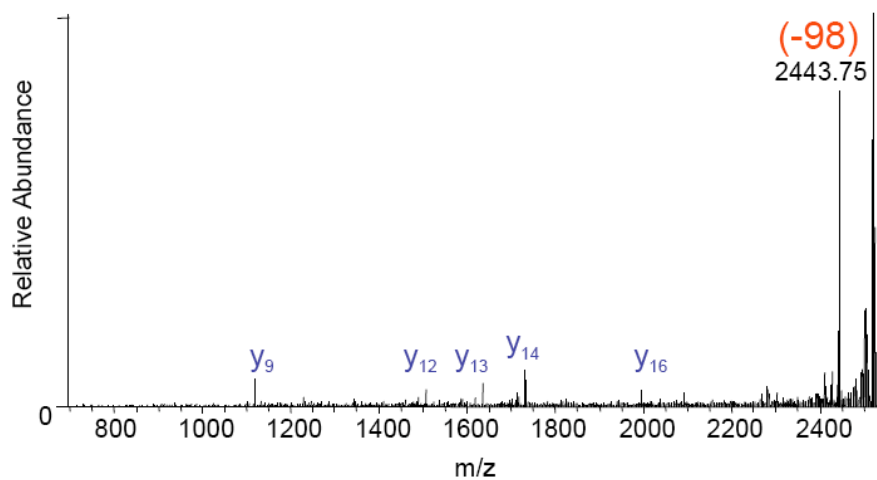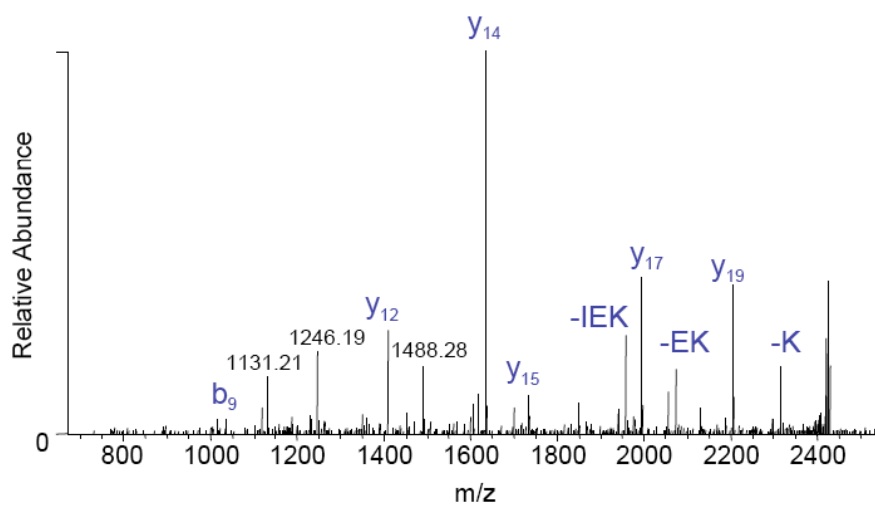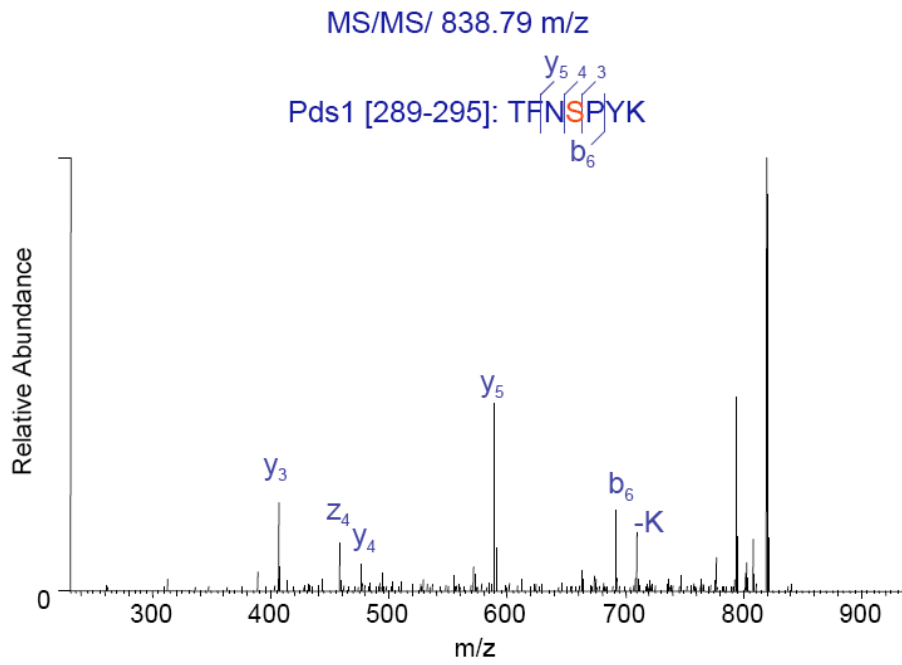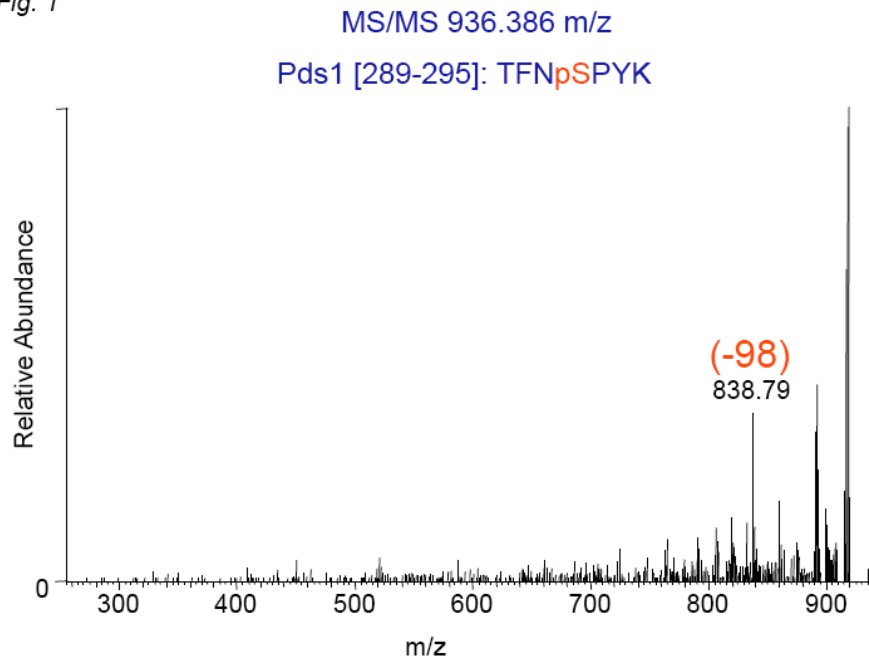
MS/MS 3192.424 m/z

Pds1 [296-322]: LDLEDEDDpTPDKVDLLPLEQIDEEGEK

MS/MS/MS 3095.13 m/z

Pds1 [296-322]: LDLEDEDDTPDKVDLLPLEQIDEEGEK
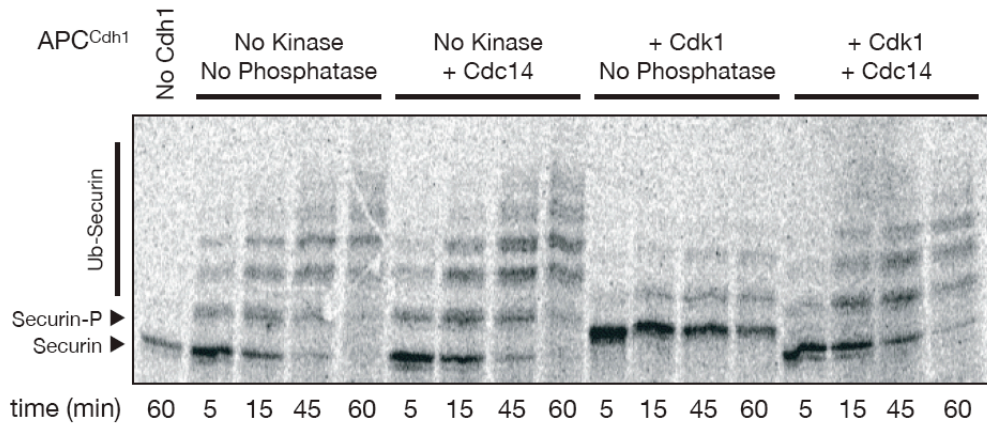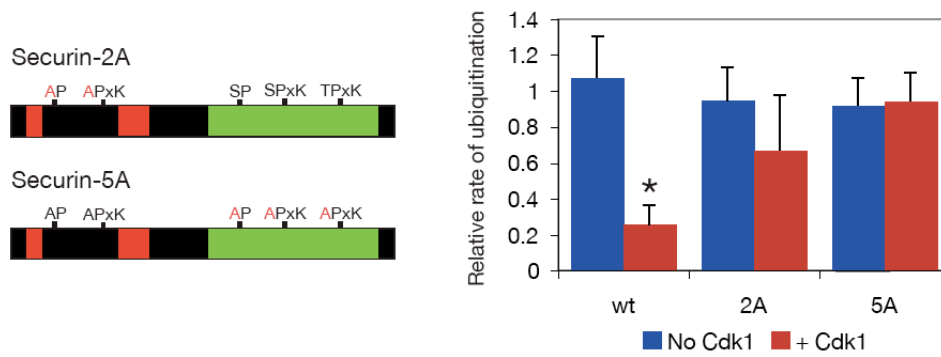
Supplementary Figure 2. Cdk1 and Cdc14 modulate the rate of securin ubiquitination by APC^Cdh1. a, ^{35}S-methionine-labeled securin was produced by translation *in vitro* and incubated with purified APC^Cdh1 and other ubiquitination components. Prior to the reactions, as indicated, some samples were incubated with either purified Clb2-Cdk1 or with Clb2-Cdk1 and then Cdc14 sequentially. The substrate was purified away from kinases and phosphatases prior t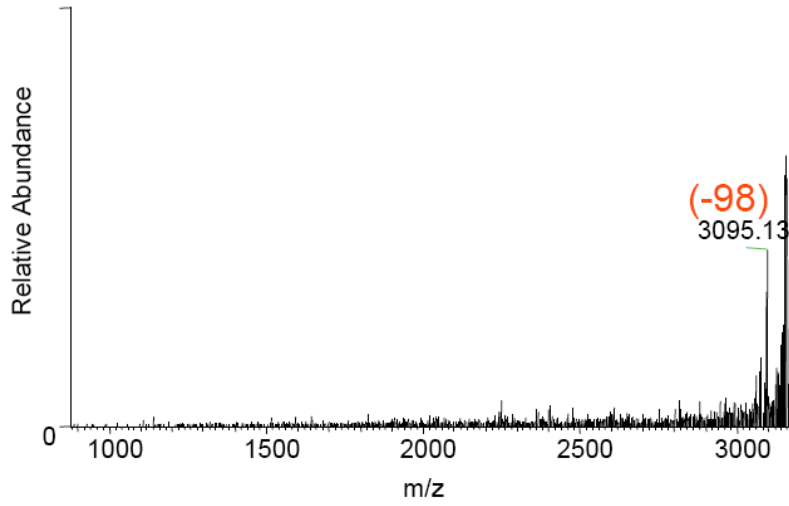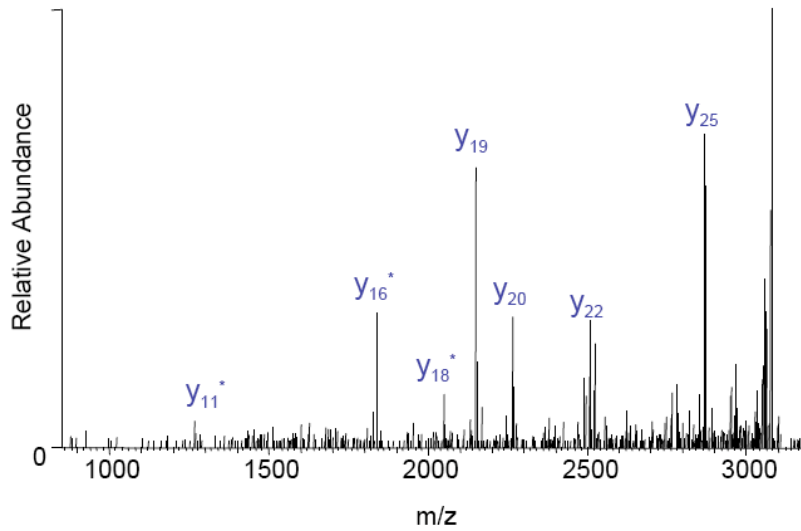o addition of APC^Cdh1. **b**, Quantitation of experiments conducted as in panel a using either wild-type securin, securin-2A, or securin-5A as a substrate. Total ubiquitination (the sum of all bands with reduced mobility) was used for the quantitation. Error bars indicate standard deviation from 3 experiments. Asterisks indicate a t-test P-value of <0.05 when comparing results with and without kinase.
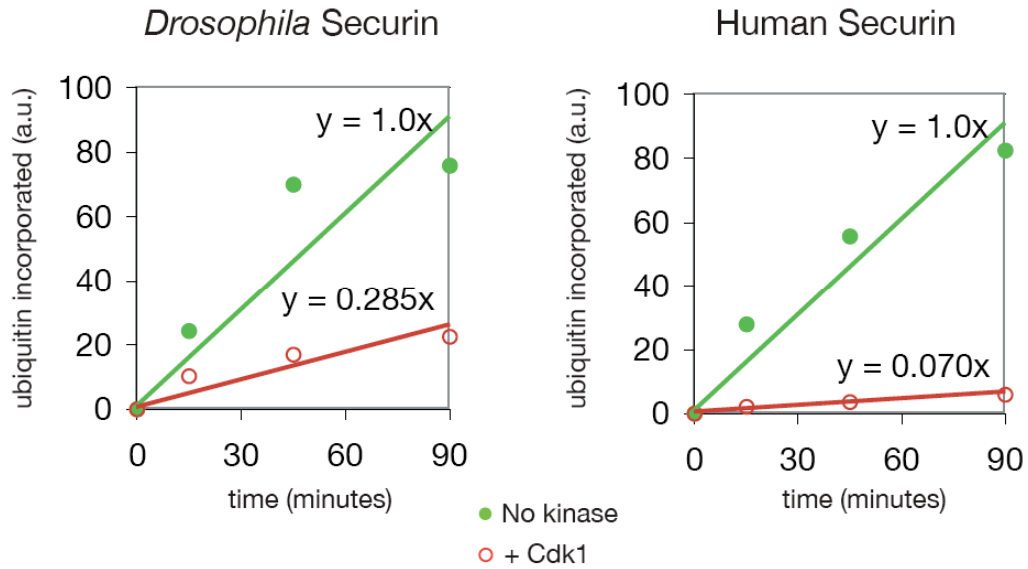
Supplementary Figure 3. Cdk1 phosphorylates *Drosophila* and human securin and modulates the rate of securin ubiquitination. Securin homologs were cloned into vectors with a T7 promoter. ^{35}S-methionine-labeled securin was produced by translation *in vitro* and incubated with purified APC[Cdh1] and other ubiquitination components. Prior to the reactions, as indicated, some samples were incubated with purified Clb2-Cdk1. The substrate was purified away from kinases and phosphatases prior to addition of APC[Cdh1]. Total ubiquitination was quantified and plotted as a function of time.

a
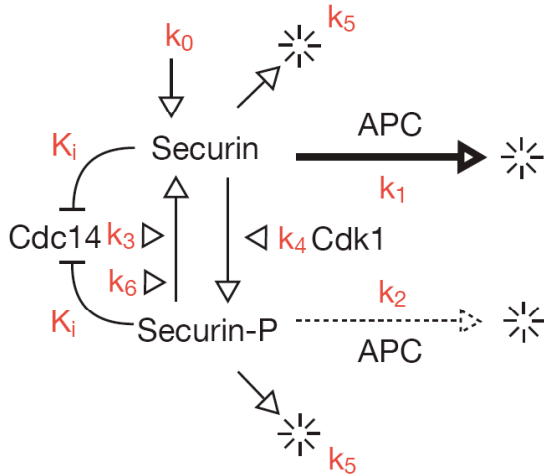
k_0 = rate of securin production

k_1 = rate of securin destruction by APC

k_2 = rate of securin-P destruction by APC

k_3 = rate of securin-P dephosphorylation by Cdc14

k_4 = rate of securin phosphorylation by Cdk1

k_5 = rate of non-specific securin destruction

k_6 = rate of non-specific securin-P dephosphorylation

K_i = IC$_{50}$ for Cdc14
note: to simplify the system the following:

Securin ⊣ Separase ⟶ Cdc14

is substituted with the steady-state equivalent:

Securin ⊣ Cdc14

m = hill coefficient for APC destruction of Securin

n = hill coefficient for Cdc14 activation

Eq. 1 $$\frac{d[\text{Securin}]}{dt} = k0 - [\text{Securin}]*k1*[\text{APC}]^m - k4*[\text{Cdk1}]*[\text{Securin}] + [\text{Securin-P}]*\left(\frac{[\text{Cdc14}]}{1+[\text{Securin-TOTAL}]^n/Ki^n}\right)*k3 - [\text{Securin}]*k5 + [\text{Securin-P}]*k6$$

Eq. 2 $$\frac{d[\text{Securin-P}]}{dt} = k4*[\text{Cdk1}]*[\text{Securin}] - [\text{Securin-P}]*k2*[\text{APC}]^m - [\text{Securin-P}]*\left(\frac{[\text{Cdc14}]}{1+[\text{Securin-TOTAL}]^n/Ki^n}\right)*k3 - [\text{Securin-P}]*k5 - [\text{Securin-P}]*k6$$

b

○ System intact
○ No phosphoregulation
○ Constitutive phosphorylation

fold inhibition = 10

c

d

Going Down

fold inhibition = 100

Going up

14
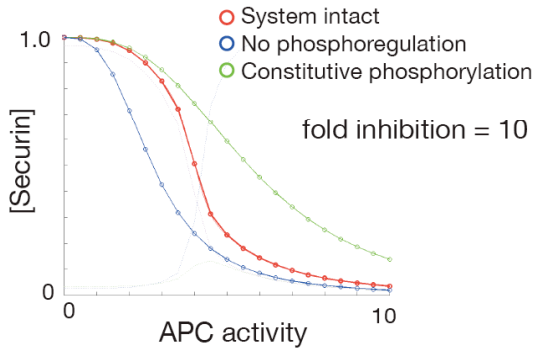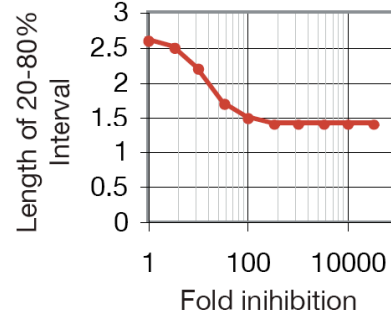
Supplementary Figure 4. Details of the mathematical model from Fig. 2. **a**, A network diagram for the model – constants are defined in the box to the right. Note that for simplicity, the destruction of cyclins is not considered in this model because adding a term for cyclin destruction does not significantly change the general behavior of the system (see Suppl. Fig. 5). Parameters used in Fig. 2: $k_0 = 10$, $k_1 = 0.01$, k_2 was varied between 0.01 and 0.000001, $k_3 = 50$, $k_4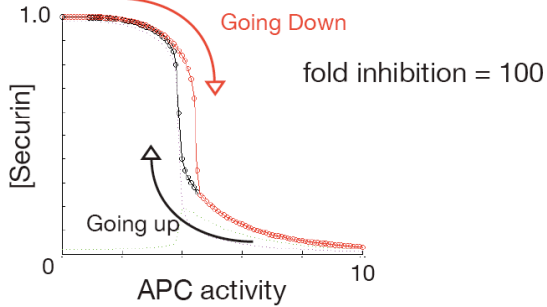 = 50$, $k_5 = 0.2$, $k_6 = 0.2$, $m = 3$, $n = 3$, $K_i = 20$. Maximum [Securin] was normalized to 1 for presentation purposes. To simplify the wiring diagram, securin directly inhibits Cdc14 activity rather than inhibiting separase, which would then activate Cdc14. Eq. 1 and Eq. 2 are the two ordinary differential equations that describe the simplified system. **b**, Simulations comparing an intact positive feedback loop to situations with no phosphorylation of securin ($k_4 = 0$) or with constitutive securin phosphorylation ($k_3 = 0$, $k_6 = 0$). Too much or too little phosphorylation makes securin degradation less abrupt. **c**, Plot of the length of the 80% - 20% interval (the change in APC activity required to reduce securin levels from 80% to 20%, a measure of the abruptness of securin degradation – the shorter the interval, the more abrupt the slope) as a function of the fold inhibition of ubiquitination upon securin phosphorylation. **d**, The system displays hysteresis, a hallmark of bistability – the response of securin levels to APC activity is different depending on the initial conditions. The red line traversing from left to right indicates the securin concentrations that result if the initial condition is low APC activity and thus high levels of securin. In this situation an abrupt drop in securin levels occurs at slightly higher levels of APC activity than the abrupt increase in securin levels that occurs when the initial condition is high APC activity and low securin (black line, traversing right to left). The labels 'Going down' and 'Going up' refer to securin concentrations.

eq 3: $[Cdk1] = C - \frac{1}{2} C * \left(\frac{[APC]^m}{K_{cdk} + [APC]^m} \right)$
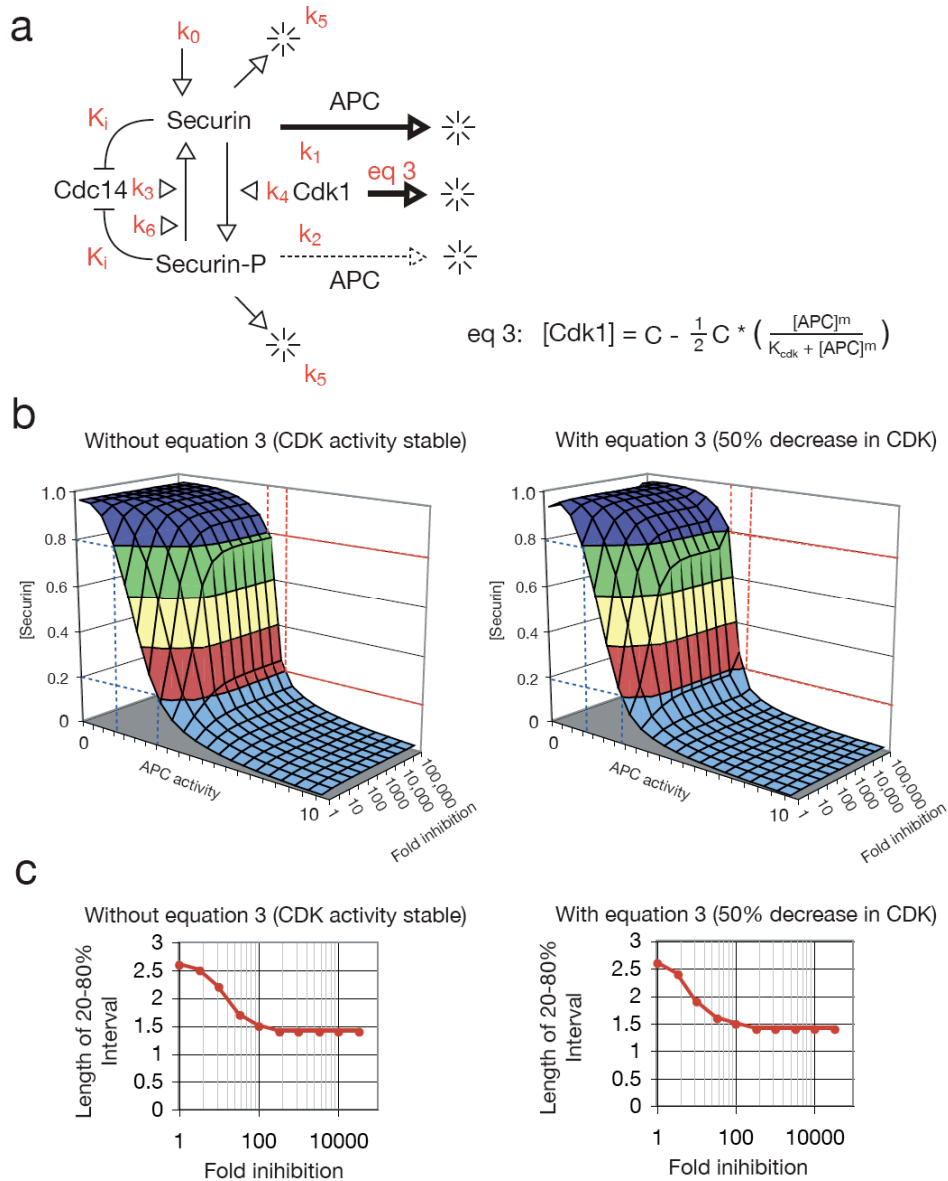
Supplementary Figure 5. Adding a term for cyclin destruction does not affect the general behavior of the model for securin destruction. **a**, A network diagram for the expanded model. The model and constants are the same as in Suppl. Fig. 4, except that a term for cyclin destruction is added (Eq. 3, where C is the maximal Cdk1 activity, and a term is defined that causes loss of 50% of Cdk1 activity as the concentration of APC is increased. $K_{cdk} = 2$). The model was also evaluated with complete loss of Cdk1 activity with similar results (not shown). **b**, A set of numerical solutions to the model in panel a, showing the steady-state levels of securin remaining (y-axis) as APC activity is varied (x-axis) when securin ubiquitination is inhibited to various degrees by phosphorylation (z-axis; see Suppl. Fig. 4 for details of model), either with (right) or without (left) cyclin destruction. **c**, Plot of the length of the 80% - 20% interval as a function of the fold inhibition of ubiquitination upon securin phosphorylation, either with (right) or without (left) cyclin destruction.

16

a

time after alpha-factor release (min)

0 15 30 45 60 75 90 105 120
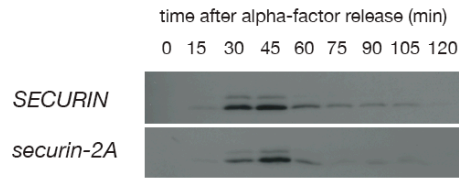
SECURIN

securin-2A

b
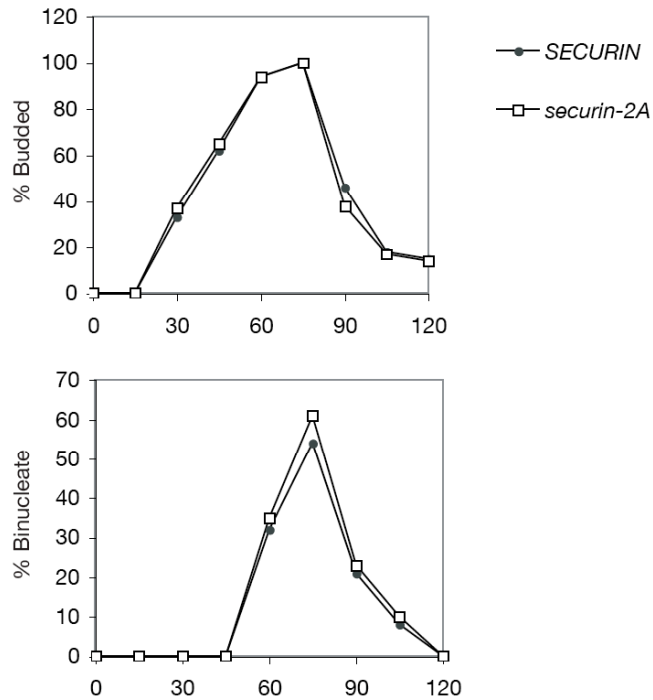
Supplementary Figure 6. The kinetics of securin-HA3 vs. securin-2A-HA3 accumulation and degradation appear to be similar in population assays. **a**, Western blot comparing securin-HA3 and securin-2A-HA3 levels in cells released from a G1 arrest by alpha-factor. **b**, Quantitation of budding and binucleate formation in the same experiment.
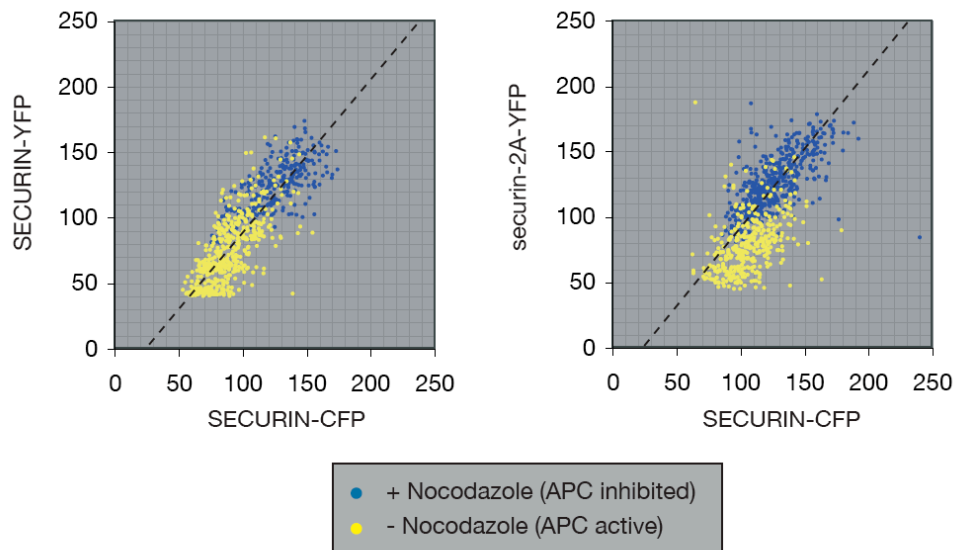
Correlation Coefficients

YFP CFP	Securin Securin	Securin securin-2A
+Nocodazole	0.7	0.68
- Nocodazole	0.7	0.43

Supplementary Figure 7. Mutation of securin's N-terminal Cdk1 consensus sites increases the efficiency of APC-dependent destruction *in vivo.* Expression of securin was induced in diploid cells of the genotype *trp1-1::P$_{GAL1}$-SECURIN-YFP-TRP1/trp1-1::P$_{GAL1}$-SECURIN-CFP-TRP1* (left) or *trp1-1::P$_{GAL1}$-securin-2A-YFP-TRP1/trp1-1::P$_{GAL1}$-SECURIN-CFP-TRP1* (right) by addition of galactose to the media for 3 h. In one culture (blue dots), 15 mg ml^{-1} nocodazole was added to activate the spindle-assembly checkpoint and inhibit APC activity. In a parallel culture (yellow dots), nocodazole was not added; in these cells, most cells were arrested or delayed in late mitosis, presumably with active APC^{Cdc20}, by the overproduced securin proteins. Cells were fixed for 1 min on ice in 4% formaldehyde, stained with DAPI and analysed by fluorescence microscopy. Micrographs were acquired with a Zeiss Axiovert-200M microscope and a Hamamatsu Orca-ER CCD camera controlled by mManager acquisition software (Vale lab, UCSF; www.micro-manager.org). Images were analysed in ImageJ using a custom Macro to quantify nuclear YFP and CFP fluorescence intensities in individual cells. The nucleus was defined by DAPI staining. In the right panel, when comparing securin-2A-YFP (y-axis) to securin-CFP (x-axis), scatter to the bottom right in the absence of nocodazole is due to cells having lower steady-state levels of securin-2A than wild-type Securin. The preferential reduction in securin-2A levels also decreases the correlation of YFP and CFP signals (table, bottom). The effects of the securin-2A mutation are suppressed by nocodazole, suggesting that they depend on APC activity.

a

b

time after addition
of tetracycline (s)
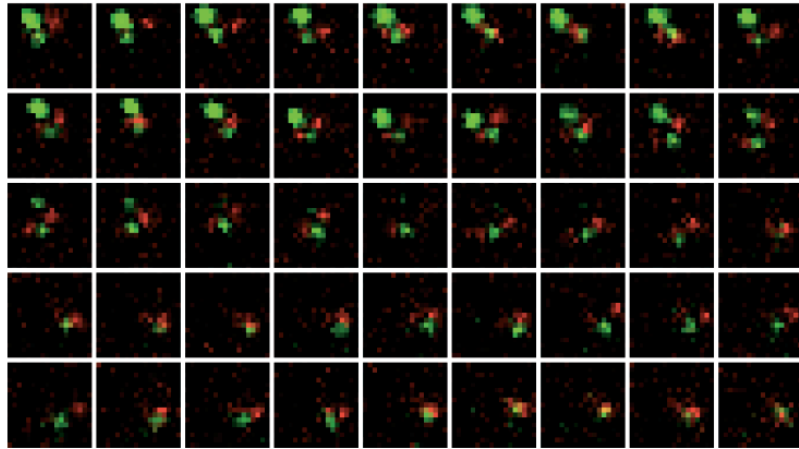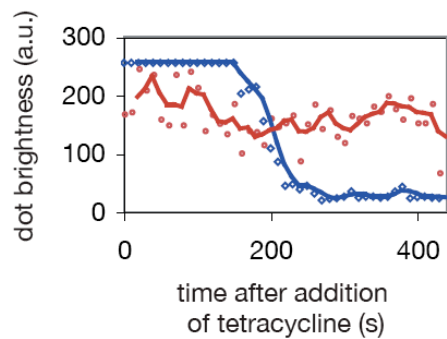
Supplementary Figure 8. The brighter GFP-dot corresponds to chromosome V. **a**, Montage from a time-lapse movie of cells to which tetracycline (200 mg/ml) was added to the medium at t_0. After about a 3 minute delay, the brighter dot rapidly disappeared, indicating that the bright dot corresponds to the *ura3-1::112xTETO-TRP1* locus on chromosome V. The dimmer dot is not affected by addition of tetracycline, indicating that it corresponds to *trp1-1::256xLACO-URA3* on chromosome IV. **b**, Quantitation of data from the experiment in panel a. Brightness is defined as the maximum pixel intensity of the dot.
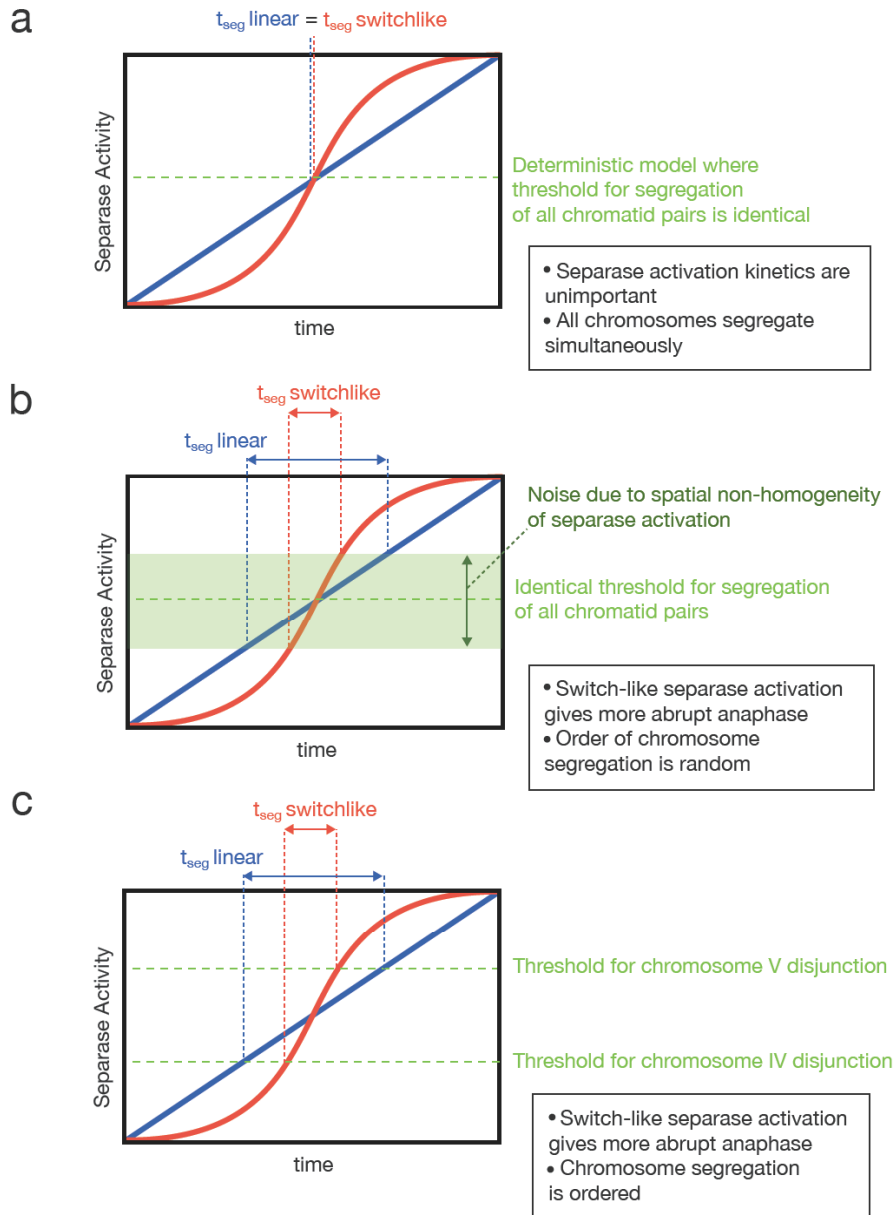
Supplementary Figure 9. Models for the disjunction of different chromatid pairs as separase activity increases. a, If all sister chromatid pairs disjoin at a single threshold of separase activity and there is no noise in the system, all chromatids will segregate simultaneously and the system is insensitive to the activation kinetics of separase. **b,** If there is a single threshold of separase activity at which all chromatids segregate but there is noise in the system, a more switch-like activation will reduce the time-lag between segregation of any two chromatid pairs. In this model, however, there is no defined order of chromatid segregation. **c,** If each chromatid pair segregates at a distinct threshold of separase activity (for example if one chromatid pair has more cohesin than another), then chromatid segregation will be ordered *and* a more switch-like activation will reduce the time-lag between segregation of any two chromatid pairs.